Available online at www.sciencedirect.com
SCIENCE DIRECT
ELSEVIER
Journal of Environmental Radioactivity 82 (2005) 21–32
JOURNAL OF ENVIRONMENTAL RADIOACTIVITY
www.elsevier.com/locate/jenvrad

Self-calibration techniques of underwater gamma ray spectrometers

D.S. Vlachos*

Hellenic Center for Marine Research, PO Box 713, Anavyssos, GR 19013, Greece

Received 23 January 2004; received in revised form 5 November 2004; accepted 24 November 2004

Abstract

In situ continuous monitoring of radioactivity in the water environment has many advantages compared to sampling and analysis techniques but a few shortcomings as well. Apart from the problems encountered in the assembly of the carrying autonomous systems, continuous operation some times alters the response function of the detectors. For example, the continuous operation of a photomultiplier tube results in a shift in the measured spectrum towards lower energies, making thus necessary the re-calibration of the detector. In this work, it is proved, that when measuring radioactivity in seawater, a photo peak around 50 keV will be always present in the measured spectrum. This peak is stable, depends only on the scattering rates of photons in seawater and, when it is detectable, can be used in conjunction with other peaks (^{40}K and/or ^{208}Tl) as a reference peak for the continuous calibration of the detector.

PACS: 29.30.Kv; 29.40.Mc

Keywords: Marine radioactivity; NaI(Tl) detector

* Tel.: +30 2910 76410; fax: +30 2910 76323.
E-mail address: dvlachos@ncmr.gr

0265-931X/$ - see front matter © 2005 Elsevier Ltd. All rights reserved.
doi:10.1016/j.jenvrad.2004.11.004

1. Introduction

In the last decades the systematic control of radioactive pollution of the seawater has been made an urgent matter. The marine environment may receive radioactive inputs via nuclear reactors or/and via nuclear accidents from neighboring countries. The natural radiation that can be measured in the seawater comprises the ^{40}K and the decay products of the ^{238}U and ^{232}Th series, most notably the ^{214}Bi, ^{214}Pb and ^{208}Tl isotopes. The measurable anthropogenic radioactivity in the seawater concerns mainly the following gamma emitters: ^{137}Cs, ^{134}Cs, ^{99m}Tc (from ^{99}Mo) and ^{60}Co (Livingston and Povinec, 2000).

The method widely used for the measurement of radionuclide concentration in the marine environment is the off-line analysis. Samples of water masses are taken from the field and chemical and pre-concentration processes are applied. The real-time radioactivity measurements in sea face considerable difficulties but also exhibit many advantages compared to the off-line method (Povinec et al., 1996). The difficulties are focused mainly on the development of detection systems with specifications appropriate for real-time measurements and a facility for direct data transfer to laboratories for further analysis. An acceptable sensor device is considered a system with low consumption (2 W), low cost, high efficiency (intrinsic and geometrical), good energy resolution and stability and tolerant construction for long-term monitoring at different depths. The development and improvement of measurement systems for radioactivity in the water environment is today of important scientific priority for the marine sciences and especially for the Operational Oceanography (Flemming, 1995). A lot of effort has been given the last decade to develop stationary monitoring network in order to observe the sea for radioactive contaminations and especially to detect ^{137}Cs (Aakens, 1995; Wedekind et al., 1999). NaI(Tl) based detectors are the preferable devices for applications in the marine environment since they combine high efficiency and capability of measuring in a wide energy range with the low power consumption (2 W) (Jones, 2001; Osvath et al., 1999; Osvath and Povinec, 2001).

In general, the in situ, long-term monitoring of underwater radioactivity faces two major problems. The first one is related to the output variation of the photomultiplier tube caused by the continuous operation (Wright, 2003; Bonutti et al., 1993). The variation of the photomultiplier sensitivity occurs mainly as a result of a variation in secondary emission, particularly in the last stages of the photomultiplier, where the currents are the highest. Although if light flux on the photomultiplier tube is reduced or high voltage is set off for some times (few 10 or 100 h), one could usually observe some recovery of the photomultiplier, but this recovery is limited in time and the photomultiplier falls down very fast to its condition previously to the interruption. An illustration of this effect is shown in Fig. 1, where a typical measured spectra are plotted. The experimental setup is described in Section 2. The photo peak of ^{40}K is clearly shown to move in lower channels, altering also the characteristics of the spectrum like the Full Width at Half Maximum.

The second problem, which is not faced when measuring radioactivity in the air, is the photon energy variation caused by the scattering of photons with the atoms in

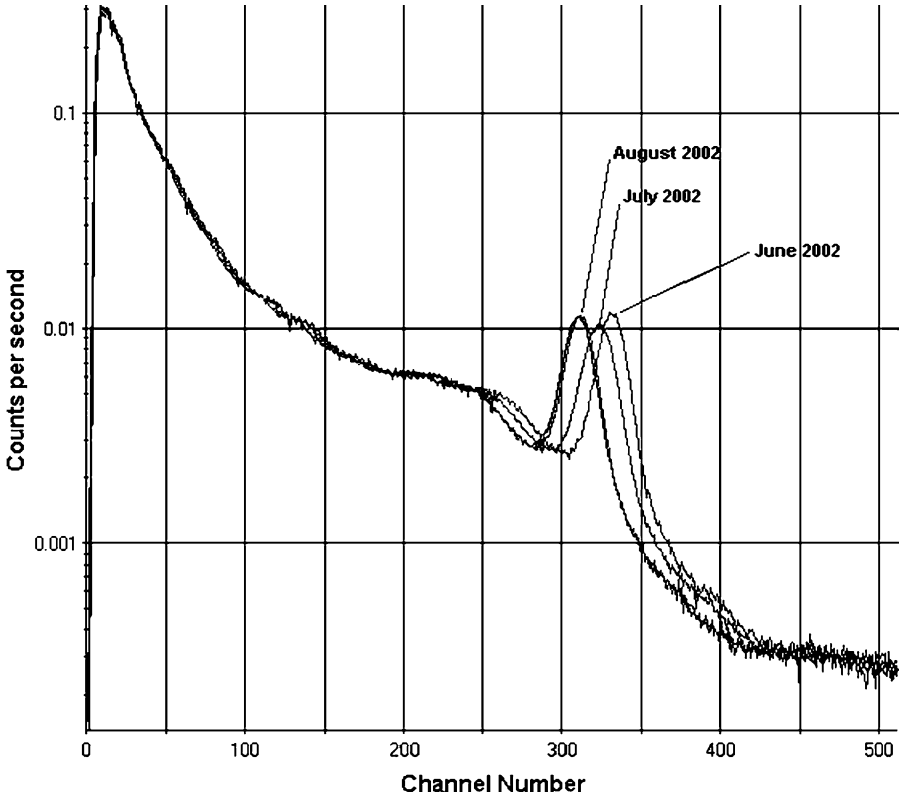

Fig. 1. Typical spectra obtained by the POSEIDON network of floating buoys. The drift of the spectrum is significant even in the short period of one month.

the seawater. Photons, after their emission and before they reach the detector, interact with seawater atoms and can change their energy due to Compton scattering or pair production, or disappear due to the photoelectric effect. Fig. 2 shows some possible scenarios for photon paths in seawater before they reach the surface of the detector. The effect of the interaction of photons with the seawater can be formulated as follow. Let $S(E)$ be the source spectrum and $M(E)$ the measured one. In air,

$$M(E) = \int_0^\infty R(E, V) S(V) \mathrm{d}V \tag{1}$$

where $R(E, V)$ is equal to the number of photons that will be recorded at energy E when one photon is emitted with energy V. The function $R(E, V)$ is known as the *transfer function* of the detector. In seawater, this relation is more complicated. If a photon with initial energy U is emitted, then there is a probability $P(V, U)$ that the

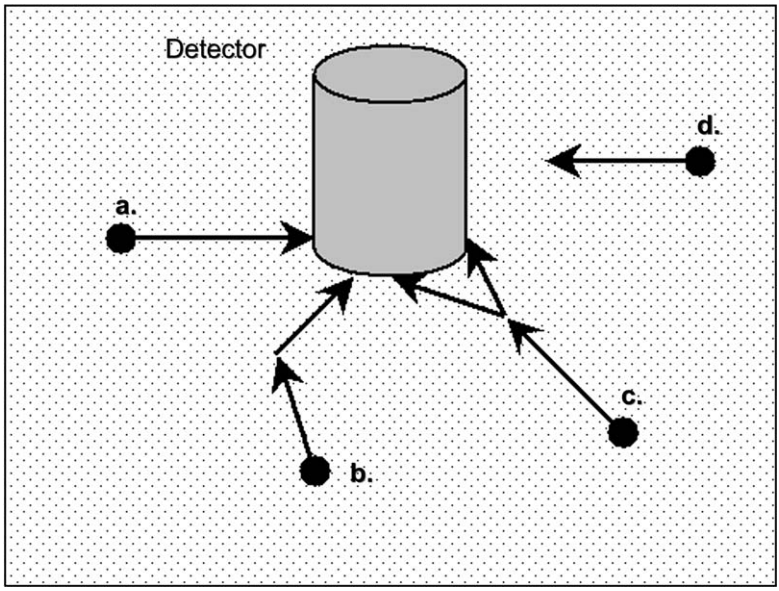

Fig. 2. Possible scenarios for photon paths in seawater. (a) The photon reaches the detector surface with no interactions. (b) The photon changes its energy and direction due to Compton scattering. (c) The photon disappears and two photons with energy 0.511 MeV are created (pair production). (d) The photon disappears due to photoelectric effect before it reaches the detector surface.

photon will reach the detector surface with a final energy V. Thus, the measured spectrum now will be given by:

$$M(E)=\int_0^\infty R(E,V)\left(\int_0^\infty P(V,U)S(U)\mathrm{d}U\right)\mathrm{d}V \tag{2}$$

Changing the order of integration in Eq. (2), the function

$$\hat{R}(E,U)=\int_0^\infty R(E,V)P(V,U)\mathrm{d}V \tag{3}$$

can be regarded now as the *modified transfer function* of the detector, for underwater operation. The measured spectrum of underwater detector can now be expressed as:

$$M(E)=\int_0^\infty \hat{R}(E,V)S(V)\mathrm{d}V \tag{4}$$

The motivation for the calculation of $P(V, U)$ is now clear. Knowing the modified transfer function of the detector, all the techniques applied to Eq. (1) for extracting information about the source spectrum, can be applied also to underwater spectra described by Eq. (4).

The analytical calculation of the function $P(V, U)$ is the objective of this work. Moreover, a method is proposed for overcoming the difficulties that arise from the spectrum shift caused by the continuous operation of the photomultiplier tube. The method uses two peaks in the measured spectrum: the one caused by the ^{40}K at 1460 keV ((Baranova et al., 2003) used this for calibration) and the other at 50 keV which will be proved that it will be always present in a spectrum measured in the marine environment.

2. Experimental

The Hellenic Center for Marine Research owns and maintains *RADAM-III* sensors constructed by the Norwegian Company OCEANOR. The detector system consists of a detector unit and a power unit shielded by an aluminum and polyester pressure tube. The detector unit is a $3'' \times 3''$ NaI(Tl) detection crystal with built-in photomultiplier tube, preamplifier, an analog–digital converter, a high voltage controller, a temperature sensor together with the electronics for data acquisition, storage and transmission. The power unit operated at DC − 12 V. The electronics modules are highly miniaturized to fit inside the sensor housing (80×60 mm) and the power consumption is very small (1 W). The operating temperature ranges between -10 and $+50$ °C and its influence to the gain shift of the detector is compensated automatically with thermistor-based hardware. The discrimination threshold of the sensor is below 20 keV.

In order to use the sensor for continuous monitoring, it has been energy calibrated and tested for its stability to temperature variations and its energy resolution. Measurements of the detector efficiency and absolute calibration in Bq/m^3 have also been performed (Tsabaris et al., 2001). For this purpose, a calibration tank of 5.5 m^3 volume, filled with water has been used. The sensor was mounted in the middle of the tank in order to be surrounded by 1 m of water, which is enough to imitate the real marine environment, due to the high attenuation of the gamma rays in the water. At the bottom of the tank an electric pump was placed in order to circulate the water to avoid sedimentation. Finally, the sensor was attached to one of the Seawatch buoys of the POSEIDON system (Soukissian et al., 2000). Fig. 1 shows typical spectra obtained in the field.

3. The distribution of photon energy in seawater

Although a large number of possible interaction mechanisms are known for gamma rays in matter, only three major types play an important role in radiation measurement: *photoelectric absorption, Compton scattering* and *pair production*. All these processes lead to the partial or complete transfer of the gamma ray photon energy to electron energy. They result in sudden and abrupt changes in the gamma-ray photon history, in that the photon either disappears entirely or is scattered through a significant angle.

In the photoelectric absorption process, a photon undergoes an interaction with an absorber atom in which the photon completely disappears. In its place, an energetic *photoelectron* is ejected by the atom from one of its bound shells. The interaction is with the atom as a whole and cannot take place with free electrons. Suppose now that in a material medium, there is a uniform in space distribution of photons. Let $n(\alpha, t)$ be the concentration of photons with energy α at time t. Each photon, undergoes a photoelectric absorption process with probability $P(\alpha)$ (P is a function of photon energy) and consequently the number of photons with energy α that disappear is $n(\alpha, t)\, P(\alpha)$. Thus:

$$\frac{\partial n(\alpha, t)}{\partial t} \propto -n(\alpha, t)P(\alpha) \tag{5}$$

The interaction process of Compton scattering takes place between the incident gamma ray photon and an electron in the absorbing material. In this mechanism, the incoming photon is deflected through an angle θ with respect to its original direction. The photon transfers a portion of its energy to the electron which is then known as a *recoil electron*. Because all angles are possible, the energy transferred to the recoil electron can vary from zero to a large fraction of the photon energy. Again, we can assign a probability $C(\alpha, \alpha')$ for a photon with initial energy α that undergoes a Compton scattering process, leaving the photon finally with energy α'. Note here that $C(\alpha, \alpha')$ is zero if $\alpha < \alpha'$ since the photon cannot gain energy. The total number of photons with initial energy α that alter their energy through the Compton scattering mechanism is $\int_0^{\alpha} n(\alpha, t)C(\alpha, v)\mathrm{d}v$. On the other hand, the total number of photons that result in energy α through the same mechanism is $\int_{\alpha}^{\infty} n(v, t)C(v, \alpha)\mathrm{d}v$. Consequently

$$\frac{\partial n(\alpha, t)}{\partial t} \propto \int_{\alpha}^{\infty} n(v, t)C(v, \alpha)\mathrm{d}v - \int_0^{\alpha} n(\alpha, t)C(\alpha, v)\mathrm{d}v \tag{6}$$

Finally, the interaction process of pair production occurs in the field of a nucleus of the absorbing material and corresponds to the creation of an electron–positron pair at the point of complete disappearance of the incident photon. Because an energy of $2m_0c^2$ (m_0 is the electron rest mass and c the speed of light) is required to create the electron–positron pair, a minimum gamma ray energy of 1.022 MeV is required to make the process energetically possible. The excess photon energy appears in the form of kinetic energy shared by the electron–positron pair. Once the positron's kinetic energy becomes very low, it will annihilate or combine with a normal electron in the absorbing medium. At this point, both disappear, and they are replaced by two annihilation photons of energy m_0c^2 (0.511 MeV). Again we can assign a probability $R(\alpha)$ that a photon with energy α disappears due to the pair production interaction. Thus, the total number of photons that disappear is $n(\alpha, t)\, R(\alpha)$. On the other hand, a number of photons with energy m_0c^2 will be created. Using a dimensionless representation for the energy (α = Photon energy/m_0c^2), the number of photons that are created is $2\delta(a-1)\int_2^{\infty} n(v, t)R(v)\mathrm{d}v$. Consequently

$$\frac{\partial n(\alpha,t)}{\partial t} \propto 2\delta(a-1)\int_2^{\infty} n(v,t)R(v)\mathrm{d}v - n(\alpha,t)R(\alpha) \tag{7}$$

In equilibrium, $n(\alpha, t)$ is independent of time. Combining Eqs. (1), (2) and (3), the photon energy distribution can be described by the following equation:

$$0=\sum_i G^i\delta\left(\alpha-\alpha_0^i\right)+\int_0^{\infty} n(v)C(v,\alpha)\mathrm{d}v+2\delta(\alpha-1)\int_0^{\infty} n(v)R(v)\mathrm{d}v-n(\alpha)S(\alpha) \tag{8}$$

where $G^i\delta(\alpha-\alpha_0^i)$ is the generation of photons at energy α, when G^i photons per second are generated with energy α_0^i. This term is necessary to account for the radioactive sources. The term $S(\alpha)$ collects all the mechanisms that alter the energy of a photon and is given by:

$$S(\alpha)=P(\alpha)+R(\alpha)+\int_0^{\alpha} C(\alpha,v)\mathrm{d}v \tag{9}$$

Eq. (4) is linear in the sense that if n_1 is the photon energy distribution caused by a source that emits photons with energy α_0^1 and n_2 is the photon energy distribution caused by a source that emits photons with energy α_0^2, then if both sources are present, the photon energy distribution will be $n_1 + n_2$. Consequently, it is adequate to solve Eq. (4) for a single source that emits at energy α_0, G photons per unit time and unit volume.

Due to the existence of the delta functions in Eq. (4), the solution can be written as:

$$n(\alpha)=\lambda(\alpha)+k\delta(\alpha-\alpha_0)+m\delta(\alpha-1) \tag{10}$$

where $\lambda(\alpha)$ is a smooth function of energy α with $\lambda(\alpha) = 0$ when $\alpha = \alpha_0$. Substituting the expression for $n(\alpha)$ in Eq. (4), we can calculate the coefficients k and m as follow:

$$k=\frac{G}{S(\alpha_0)} \tag{11}$$

$$m=2\times\frac{kR(\alpha_0)+\int_0^{\infty}\lambda(v)R(v)\mathrm{d}v}{S(1)} \tag{12}$$

Substituting the results from Eqs. (8), (9) and (10) in Eq. (4), the delta functions are eliminated and the resulting equation for $\lambda(\alpha)$ is:

$$\frac{GC(\alpha_0,\alpha)}{S(\alpha_0)}+2\times\frac{\frac{G}{S(\alpha_0)}R(\alpha_0)+\int_0^{\infty}\lambda(v)R(v)\mathrm{d}v}{S(1)}C(1,\alpha)+\int_0^{\infty}\lambda(v)C(v,\alpha)\mathrm{d}v-\lambda(\alpha)S(\alpha)=0 \tag{13}$$

For the numerical solution, the functions $R(v)$ and $S(\alpha)$ are calculated from XCOM software (Berger and Hubell, 1995). The function $C(v, \alpha)$ is calculated from the Klein–Nishina formula (Tsoulfanidis, 1983) which gives for the angular distribution of scattered photons:

$$p(\theta)=C_M\pi r_0^2\left(\frac{v}{\alpha}\right)^2\left(\frac{v}{\alpha}+\frac{\alpha}{v}-\sin^2\theta\right),\quad v=\frac{\alpha}{v+\alpha(1-\cos\theta)} \tag{14}$$

where α is the initial photon energy, v the resulting photon energy after the scattering, r_0 the classical electron radius and C_M is a constant that depends on the absorbing medium and is related to the density of scattering centers. Changing now the variable from θ to v we get

$$C(\alpha,v)=C_m\pi r_0^2\frac{1}{\alpha^2}\left[\frac{v}{\alpha}+\frac{\alpha}{v}-1+\left(1-\frac{1}{v}+\frac{1}{\alpha}\right)^2\right]\left[u\left(v-\frac{\alpha}{v+2\alpha}\right)-u(v-\alpha)\right] \tag{15}$$

where u is the step function, whose role is to ensure that the scattered photon can neither increase its energy nor results in an energy lower than the Compton edge. Fig. 2 shows the calculated photon distribution for different values of α_0 with $G = 1$.

The interesting point that comes out from Fig. 2 is that the distribution function has a peak at around 50 keV, independent of the initial photon energy. In order to check this theoretically, we focus the solution of Eq. (11) around 50 keV ($\alpha \simeq 0.1$), assuming that the initial photon energy α_0 is greater that $0.1/(1-2\times0.1)=0.125$ (around 63 keV). Under these conditions, the first and second term of Eq. (11) vanish, because $C(\alpha_0,\ \alpha)=0$ and $C(1,\ \alpha)=0$. Moreover, $R(0.1)=0$ and substituting expression (5) for $S(\alpha)$, Eq. (11) now becomes:

$$\int_0^\infty \lambda(v)C(v,\alpha)\mathrm{d}v-\lambda(\alpha)\left[P(\alpha)+\int_0^\infty C(\alpha,v)\mathrm{d}v\right]=0 \tag{16}$$

In order to calculate the location of the maximum, we notice that since $C(v, \alpha)$ in the first term of Eq. (12) is non-zero in the short interval $[\alpha, \alpha/(1-2\alpha)]$ (between 50 and 63 keV) we can substitute $\lambda(v)$ with $\lambda(\alpha)$, leading of course to a small error in the location of the peak. Taking the derivative of Eq. (12) over α and setting $\mathrm{d}\lambda(\alpha)/\mathrm{d}\alpha=0$, we get:

$$\int_0^\infty \frac{\partial C(v,\alpha)}{\partial\alpha}\mathrm{d}v-\frac{\mathrm{d}P(\alpha)}{\mathrm{d}\alpha}-\int_0^\infty \frac{\partial C(\alpha,v)}{\partial\alpha}\mathrm{d}v=0 \tag{17}$$

The solution of the above equation gives the location of the peak. Notice here that Eq. (13) depends only on the scattering rates and not on the distribution of photon energy. Eq. (13) can be rewritten as:

$$-\frac{\mathrm{d}P(\alpha)}{\mathrm{d}\alpha}=\Lambda(\alpha) \tag{18}$$

where

$$\Lambda(\alpha) = C_M \pi r_0^2 \frac{4}{\alpha^2} - C_M \pi r_0^2 \frac{1}{\alpha^2}\left(\frac{1+2\alpha+\frac{1}{1+2\alpha}}{(1+2\alpha)^2}+1-2\alpha+\frac{1}{1-2\alpha}\right) + \int_{\frac{\alpha}{1+2\alpha}}^{\alpha} C_M \pi r_0^2 \frac{1}{\alpha^2}\left(\frac{-3v}{\alpha^2}-\frac{1}{v}+\frac{2}{\alpha}+2\left(1-\frac{1}{v}+\frac{1}{\alpha}\right)\left(\frac{-1}{\alpha}+\frac{1}{v\alpha}-\frac{2}{\alpha^2}\right)\right)\mathrm{d}v - \int_{\alpha}^{\frac{\alpha}{1-2\alpha}} C_M \pi r_0^2 \frac{1}{v^2}\left(-\frac{v}{\alpha}+\frac{1}{v}+\frac{2}{\alpha^2}\left(1-\frac{1}{\alpha}+\frac{1}{v}\right)\right)\mathrm{d}v \quad (19)$$

Fig. 3 shows the graphical solution of Eq. (14). The intersection of the two plotted curves occur at the point $\alpha \simeq 50$ keV. In the same figure, the embedded plot shows the dependence of the calculated energy as a function of the salinity of the seawater.

Let us take now a closer look at the result that we extracted. Photons, as soon as they created from the radioactive source, interact with the atoms of the seawater. The main scattering mechanism, as is shown in Fig. 4, is the Compton scattering except for very low energies, where the probability of the photoelectric effect is dominant. As a result, photons are gathered in lower energies. This explains the monotonicity of the distribution of photon energies, as it is clear from Fig. 2 (except for low energies). As a consequence, at every energy, there is a flux of incoming photons from photons with higher energies that undergo Compton scattering and a flux of outcoming photons that undergo either Compton scattering or photoelectric absorption. The outcoming flux is proportional to the concentration of photons. In equilibrium, these two fluxes must be equal. But as the energy is getting lower, the probability of photoelectric absorption increases dramatically. Thus, in order that

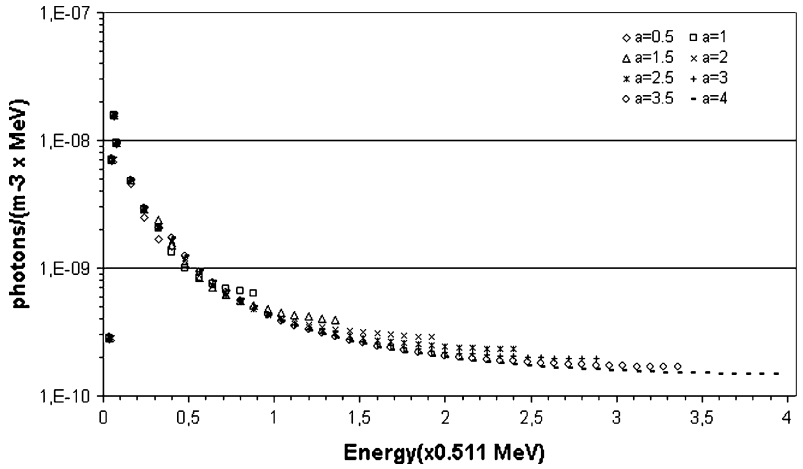

Fig. 3. Energy distribution of photons in seawater for different values of initial photon energy. The photon energy E is represented in dimensionless form, $\alpha = E/m_0c^2$, where m_0 is the electron rest mass and c the speed of light.

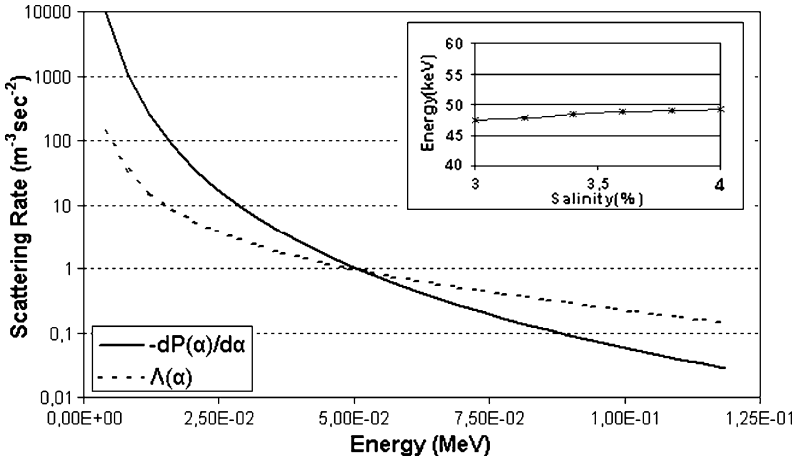

Fig. 4. Graphical solution of Eq. (14) is shown, which gives the value $E \simeq 50$ keV. The salinity of the seawater was taken to be 3.6% (characteristic for the Greek seas). In the embedded figure, the calculated peak energy is shown as a function of the salinity of the seawater.

the equality between the incoming and outcoming flux is held, the concentration of photons cannot be further increased. From this point, as the energy is getting lower, the concentration of photons decreases in order to balance the increase of the probability of the photoelectric absorption, given that the incoming photon flux does not change significantly (observe the plateau of the Compton scattering probability at low energies in Fig. 5). This is the reason why the distribution of photon energy exhibits a maximum at low energies.

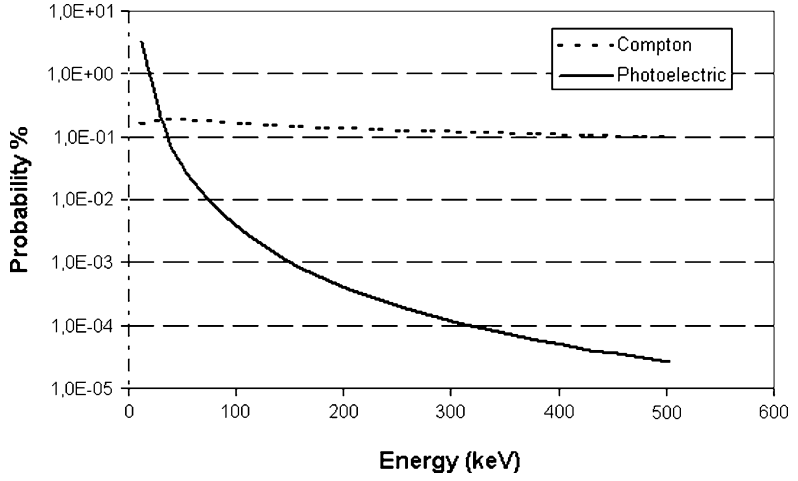

Fig. 5. Probabilities of photoelectric absorption (solid line) and Compton scattering (dashed line) in seawater with salinity 3.5%.

The existence of the photo peak at 50 keV, when it is measurable, gives an alternative to the already well known techniques (Guillot, 2001 and references there in) for the real-time continuous sensor calibration. This maximum at 50 keV in combination with the photo peak of ^{40}K at 1461 keV will always be present in a measured spectrum in seawater. The photon energy (E)–detector channel (C) relation can be expressed as: $E = aC + b$, where a is the gain and b the offset, both dependent on the amplifier and the preamplifier. Both constants can be determined by the identification of the aforementioned photo peaks. Moreover, ^{208}Tl (photo peak at 2615 keV) can be used also in order to account for detector non-linearity. In this case, the above relation becomes $E = a_1C^2 + a_2C + b$. The three peaks are adequate for the calculation of all the three constants. Note here that this technique is applicable only in cases where the measurement of the 50 keV peak is permitted by the discrimination threshold settings of the detector.

4. Conclusions

The numerical calculation of the photon energy distribution in seawater can be used for the determination of the modified transfer function of the detector (the transfer function of the detector when it is used for underwater measurements), simplifying thus the unfolding of the measured spectrum. Moreover, it has been found that the distribution of photon energy in seawater gives a local maximum at the energy of 50 keV. This maximum, which is independent on the initial photon energy, is caused by the high probability of the photoelectric effect in low energies and its value depends only on the scattering rates of photons in seawater. Finally, this peak, when it is measurable, can be used for continuous energy calibration of the detector.

References

Aakens, U.R., 1995. Radioactivity monitored from moored oceanographic buoys. Chemistry and Ecology 10, 61–69.

Baranova, I., Kharitonovb, I., Laykinc, A., Olshansky, Y., 2003. Devices and methods used for radiation monitoring of sea water during salvage and transportation of the Kursk nuclear submarine to dock. Nuclear Instruments and Methods in Physics Research A 505, 439–443.

Berger, M.J., Hubell, J.H., 1995. XCOM: photon cross sections with a personal computer, NBSIR 87-3597.

Bonutti, F., Camerini, P., Grion, N., Rui, R., Amaudruz, P., 1993. A method for monitoring the stability of photomultipliers. Nuclear Instruments and Methods in Physics Research Section A: Accelerators, Spectrometers, Detectors and Associated Equipment 337 (1), 165–170.

Flemming, N.C., 1995. Making the case for GOOS. Sea Technology, Special Feature, 44–49.

Guillot, L., 2001. Extraction of full absorption peaks in airborne gamma-spectrometry by filtering techniques coupled with a study of the derivatives. Comparison with the window method. Journal of Environmental Radioactivity 53, 381–398.

Jones, F.G., 2001. Development and application of marine gamma-ray measurements: a review. Journal of Environmental Radioactivity 53, 313–333.

Livingston, H.D., Povinec, P.P., 2000. Anthropogenic marine radioactivity. Ocean and Coastal Management 43, 689–712.

Osvath, I., Povinec, P.P., Huynh-Ngoc, L., Comanducci, J.-F., 1999. Underwater gamma surveys of Mururoa and Fangataufa lagoons. The Science of the Total Environment 237/238, 227–286.

Osvath, I., Povinec, P.P., 2001. Seabed γ-ray spectrometry: applications at IAEA-MEL. Journal of Environmental Radioactivity 53, 335–349.

Povinec, P.P., Osvath, I., Baxter, M.S., 1996. Underwater gamma-spectrometry with HPGe and NaI(Th) Detectors. Applied Radiation and Isotopes 47, 1127–1133.

Soukissian, T., Chronis, G., Poseidon Group (D. Ballas, D. Vlachos, K. Nittis, Ch. Diamanti, L. Perivoliotis, E. Papageorgiou, S. Barbetseas and A. Mallios), 2000. Poseidon: a marine environmental monitoring, forecasting and information system for the Greek Seas. Mediterranean Marine Science 1/1, 71–78.

Tsabaris, C., Vlachos, D.S., Papadopoulos, C.T., Theodonis, I., Vlastou, R., Kalfas, C.A., 2001. Development and application of an underwater gamma-ray spectrometer for radioactivity measurements. International Conference on North Aegean System Functioning and Inter-Regional Pollution, Kavala May 2001, Greece, pp. 31–38.

Tsoulfanidis, N., 1983. Measurement and Detection of Radiation. Hemisphere Publishing Corporation, ISBN 0-89116-523-1.

Wedekind, Ch., Shilling, G., Gruttmuller, M., Becker, K., 1999. Gamma-radiation monitoring network at sea. Applied Radiation and Isotopes 50, 733–741.

Wright, A.G., 2003. Amplifiers for use with photomultipliers – who needs them? Nuclear Instruments and Methods in Physics Research Section A: Accelerators, Spectrometers, Detectors and Associated Equipment, vol. 504, Issues 1–3, 21 May 2003. Proceedings of the 3rd International Conference on New Developments in Photodetection, pp. 245–249.